Available online at www.sciencedirect.com
SCIENCE DIRECT®
Journal of Power Sources 135 (2004) 262–266
JOURNAL OF POWER SOURCES
www.elsevier.com/locate/jpowsour

Electrochemical characteristics of $LiNi_{0.5}Mn_{0.5-x}Ti_xO_2$ prepared by solid state method

Decheng Li, Takahisa Muta, Hideyuki Noguchi*

Department of Applied Chemistry, Saga University, Hohjyo-1, Saga 840-8502, Japan

Received 1 September 2003; accepted 1 April 2004

Available online 2 June 2004

Abstract

$LiNi_{0.5}Mn_{0.5-x}Ti_xO_2$ series was prepared by a simple solid state method using MnO_2, TiO_2 and nickel carbonate basic as the starting materials. Its structural and electrochemical characteristics were also studied and compared with those prepared by the spray dry method. As Ti content increases, the degree of cation mixing increases and the structure of compound transforms gradually from a layered structure to a disordered rock salt structure. There are two plateaus in the initial charge curve for compounds with $x < 0.3$. One is around 4.0 V and the other is around 4.6 V. Both the initial charge and discharge capacities decrease as Ti content increases. Compounds with $x < 0.3$ exhibit good cyclic performance at room temperature.

Keywords: Li-ion battery; Cathode material; $LiNi_{0.5}Mn_{0.5-x}Ti_xO_2$; Solid state reaction; Electrochemical behavior

1. Introduction

Many efforts have been made to develop new materials as an alternative to $LiCoO_2$ due to the relative high cost and toxicity of Co [1–3]. Recently, a layered $LiNi_{0.5}Mn_{0.5}O_2$, which can be regarded as a one-to-one mixture of $LiNiO_2$ and $LiMnO_2$, has been proposed as a promising cathode material for Li-ion battery application [4]. It has many advantages over $LiNiO_2$ and $LiMnO_2$, such as its high reversible capacity, structural and thermal stability as well as excellent cyclability [5]. Nevertheless, Cushing and Goodenough [6] have reported that its poor electronic conductivity could dramatically reduce its specific capacity even at a moderate current density.

Foreign metal ion doping is a well-established method to improve the electrochemical properties of cathode materials [7]. The valence of Mn in $LiNi_{0.5}Mn_{0.5}O_2$ is determined to be tetravalent by X-ray absorption spectroscopy (XAS) [8]. Therefore, the Ti ion can substitute the Mn ion in $LiNi_{0.5}Mn_{0.5}O_2$. However, only a few studies have shown the influence of metal ion doping on the structure and electrochemical behavior of $LiNi_{0.5}Mn_{0.5}O_2$ [9–11]. This is possibly due to its difficulty in the preparation of a pure phase by the conventional solid state method [4,12]. Ni–Mn double hydroxide obtained by the co-precipitation method is usually used as the starting material. Thus, it is difficult to freely control the composition of the Li–Ni–Mn–Ti oxide.

We have prepared a $LiNi_{0.5}Mn_{0.5-x}Ti_xO_2$ series by a spray dry method [13] and found that Ti substitution for Mn could not only upgrade its electrochemical properties, but also promote the formation of the $LiNi_{0.5}Mn_{0.5-x}Ti_xO_2$. This phenomenon could also be observed in a $LiNi_{0.5-x}Mn_{0.5-x}Co_{2x}O_2$ system [14]. These results suggest that it is possible to prepare the $LiNi_{0.5}Mn_{0.5}O_2$ derivatives by conventional solid state method simply through Ti^{4+} ion doping.

In the present study, a new synthesis route was attempted to prepare the $LiNi_{0.5}Mn_{0.5-x}Ti_xO_2$ compounds. Its electrochemical behavior at high working voltage was also investigated and compared with those prepared by the spray dry method.

2. Experimental

Stoichiometrical MnO_2 (Chemical Manganese Dioxide, WS Li type, SADACEM S.A.), TiO_2 (MT-150A, Tayca Co.), and Nickel Carbonate Basic (guaranteed reagent, Wako) were thoroughly mixed and then preheated at 470 °C for 10 h in air. After adding stoichiometrical $LiOH{\cdot}H_2O$ (guaranteed reagent, Wako) into the obtained precursors, they were

* Corresponding author. Tel.: +81 952 28 8674; fax: +81 952 28 8591.
E-mail address: noguchih@cc.saga-u.ac.jp (H. Noguchi).

0378-7753/$ – see front matter © 2004 Elsevier B.V. All rights reserved.
doi:10.1016/j.jpowsour.2004.04.003

ground, sintered at 900 °C for 10 h in air and then cooled to 100 °C in furnace.

The XRD measurement was carried out using a Rigaku Rint1000 diffractometer equipped with a monochromator and Cu target tube.

Scanning electron microscope (SEM) study of the samples was performed on JEOL JSM-5200 electron microscope.

The Charge/discharge tests were carried out using the CR2032 coin-type cell, which consists of a cathode and lithium metal anode separated by a Celgard 2400 porous polypropylene film. The cathode contains a mixture of 20 mg of accurately weighted active materials and 13 mg of teflonized acetylene black (TAB-2) as the conducting binder. The mixture was pressed onto a stainless screen and dried at 170 °C for 5 h under vacuum. The cells were assembled in a glove box filled with dried argon gas. The electrolyte is 1 M $LiPF_6$ in ethylene carbonate/dimethyl carbonate (EC/DMC, 1:2 (v/v)). Cells were first charged to 4.8 V at a rate of 0.1 mA/cm^2 (10 mA/g) and held at this voltage for 3 h (called C.C.-C.V. mode) then discharged at a current density of 0.1 mA/cm^2 (10 mA/g).

Cyclic Voltammetry study was carried out by means of tri-electrode cell, using metal lithium as counter and reference electrodes and 1 M $LiPF_6$ in ethylene carbonate/dimethyl carbonate (EC/DMC, 1:2 (v/v)) as the electrolyte. Cell was operated at a scan rate of 0.05 mV/s in the voltage range of 3–4.8 V versus Li/Li$^+$. The area of the working electrode is about 0.75 cm^2.

3. Results and discussion

Fig. 1 shows the XRD patterns of $LiNi_{0.5}Mn_{0.5-x}Ti_xO_2$ ($0 \le x \le 0.5$) synthesized at 900 °C. All peaks are sharp and well-defined, suggesting that compounds are well-crystallized. Trace amount of impurity, NiO, were found in all samples except for $x = 0.15$ and 0.5. In the case of $LiNi_{0.5}Mn_{0.5-x}Ti_xO_2$ prepared by the spray dry method, 0.04 mol Ti substitution for Mn is enough to ensure the formation of $LiNi_{0.5}Mn_{0.5-x}Ti_xO_2$ with a high purity [13]. The presence of unreacted NiO phase in compounds prepared by solid state method would be due to the uniformity of metal ion distribution in precursors, since the starting materials can be homogeneously mixed at an atomic level by means of the spray dry method. Moreover, compounds with $0 \le x \le 0.3$ have a layered structure and main peaks can be indexed on the α-$NaFeO_2$ structure (space group R3 m). The unit cell would expand as x increases since all peaks of sample shift to a lower angle as x increases. The intensity of the (0 0 3) and (1 0 1) peaks gradually decreases while the intensities of the (1 0 2) and (1 0 4) peaks increase relatively with an increase in x value. This result suggests that the degree of cation mixing becomes severe at high Ti contents, because the intensity ratio of I_{003}/I_{004} is sensitive to the cation distribution in the lattice [15]. The XRD pattern of the compound with $x > 0.4$, is similar to that of rock-salt typed α-$LiFeO_2$. Therefore, the layered structure transforms completely to a disordered rock-salt like structure by the substitution of Ti for Mn in $LiNi_{0.5}Mn_{0.5}O_2$.

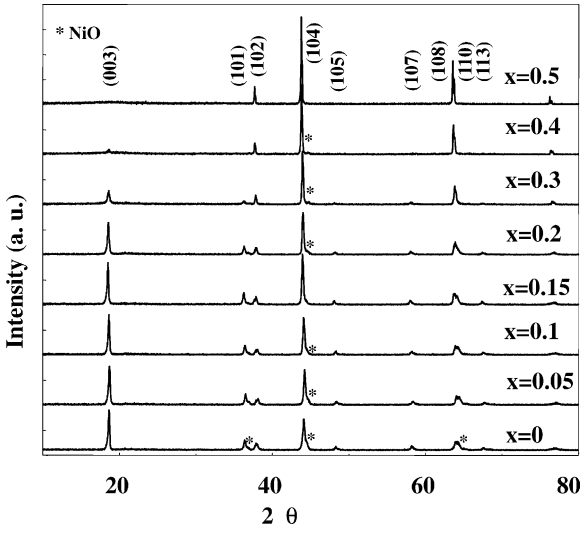

Fig. 1. XRD patterns of $LiNi_{0.5}Mn_{0.5-x}Ti_xO_2$ ($0 \le x \le 0.5$) synthesized at 900 °C.

Fig. 2 demonstrates the relation between the lattice parameters of $LiNi_{0.5}Mn_{0.5-x}Ti_xO_2$ and Ti content, x. The lattice parameters of $LiNi_{0.5}Mn_{0.5-x}Ti_xO_2$ prepared by the spray dry method were also indicted as a reference. In general, the trend of the lattice parameters, a and c, of $LiNi_{0.5}Mn_{0.5-x}Ti_xO_2$ prepared by the new route is same as that by the spray dry method. In other words, the values of lattice parameters initially increase with the increase in x for $x \le 0.3$ and keep constant values. However, both lattice parameters, a and c, of $LiNi_{0.5}Mn_{0.5-x}Ti_xO_2$ with $x \le 0.3$ prepared by the new route are always smaller than those by the spray dry method. The smaller lattice parameters are probably due to the presence of impurity phase. As the lattice constant, a, increases as a function of x, Ti doping causes an increase in the average metal–metal intra-sheet distance and further enlarges the lattice volume, V. This is probably related to the larger ionic radius of Ti^{4+} (0.68 Å, six coordination data) than Mn^{4+} (0.60 Å, six coordination data) [16]. The lattice constant, c, initially rapidly increases and then remains constant at ca. 14.32 Å for $x > 0.2$. The trigonal distortion, c/a, keeps a constant value of 4.94–4.95 for layered compounds with $x \le 0.3$ and keeps a lower value of 4.90–4.92 for rock-salt type compounds. This value is very close to 4.90 of ideal close cubic packed compound.

Fig. 3 shows the initial charge-discharge curves of $LiNi_{0.5}Mn_{0.5-x}Ti_xO_2$ ($0 \le x \le 0.3$) within the voltage range of 3–4.8 V at room temperature. The initial charge and discharge capacities of samples with $0.05 \le x \le 0.15$ are larger than those of $LiNi_{0.5}Mn_{0.5}O_2$, consistent well with the case of $LiNi_{0.5}Mn_{0.5-x}Ti_xO_2$ prepared by the spray dry method [13]. Kang et al. [9] have reported that the substitution of Ti increases the discharge capacity from 120 mAh/g for

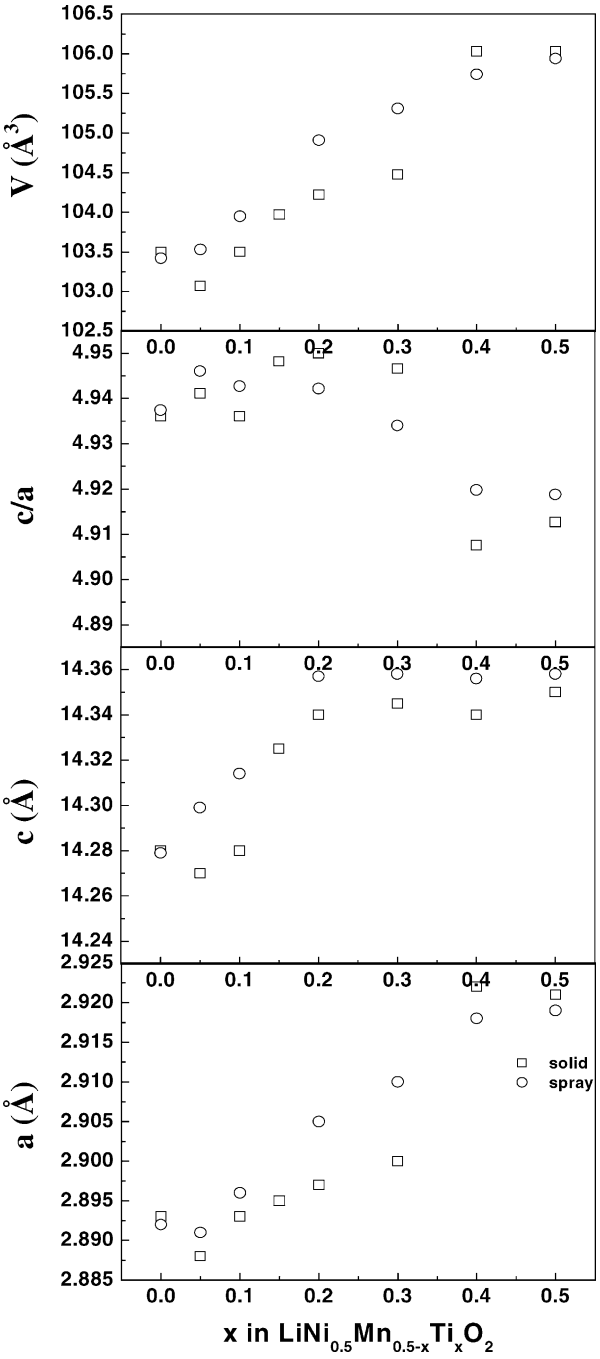

Fig. 2. Relation between the lattice parameters of $LiNi_{0.5}Mn_{0.5-x}Ti_xO_2$ and Ti content, x.

$LiNi_{0.5}Mn_{0.5}O_2$ to 132 mAh/g for $LiNi_{0.475}Mn_{0.475}M_{0.05}O_2$ at a current density of 0.1 mA/cm^2 in 3–4.3 V. Nevertheless, both the charge and discharge capacities decrease as x increases. This degradation is probably related to the increase of cation mixing degree.

It is interesting to note that there are two plateaus in all initial charge curves. One is around 4.0 V and the other is around 4.6 V. Fig. 4 shows the differential capacity vs. voltage curves of $LiNi_{0.5}Mn_{0.4}Ti_{0.1}O_2$ prepared by two methods. The peak around 4.5 V is merely appearing in the curve of sample prepared by solid state method. Yoshio et al. [17] have reported that the impurity phase, NiO, could be observed in the products of $Li_yMn_xNi_{1-x}O_2$ prepared by solid state method, because of the preferential formation of Li_2MnO_3. Thus, we believe that the presence of residual NiO in our samples suggests the formation of a solid solution system, such as a layered compound of Li–Ni–Ti–O with Li_2MnO_3 (i.e. $LiNi_{0.5}Mn_{0.5-x}Ti_xO_2$–$Li_2MnO_3$) or Li–Ni–Mn–O with Li_2TiO_3 (for example, $LiNi_{0.5}Mn_{0.5}O_2$–Li_2TiO_3). This assumption is reasonable since Kim et al. [10] have observed

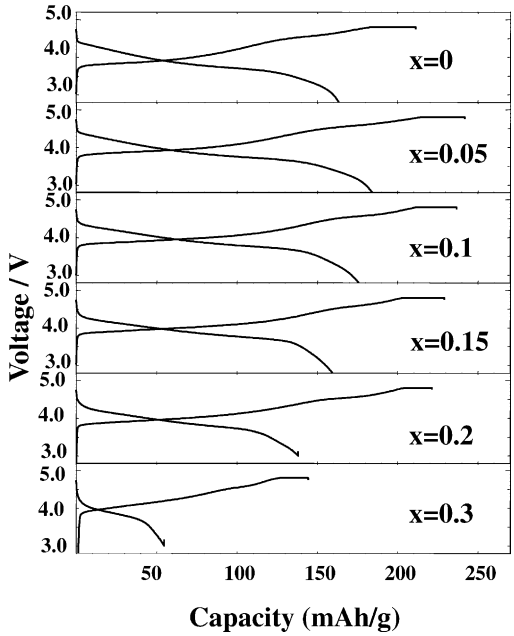

Fig. 3. Initial charge/discharge curves of $LiNi_{0.5}Mn_{0.5-x}Ti_xO_2$ cycled at room temperature.

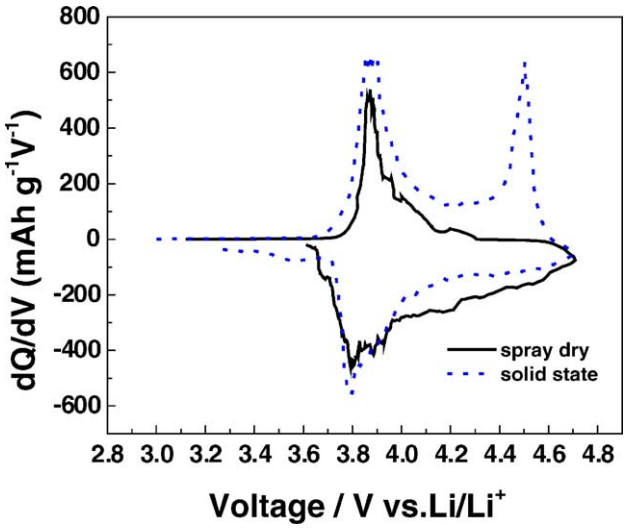

Fig. 4. Differential capacity vs. voltage curves of $LiNi_{0.5}Mn_{0.4}Ti_{0.1}O_2$ prepared by two methods.

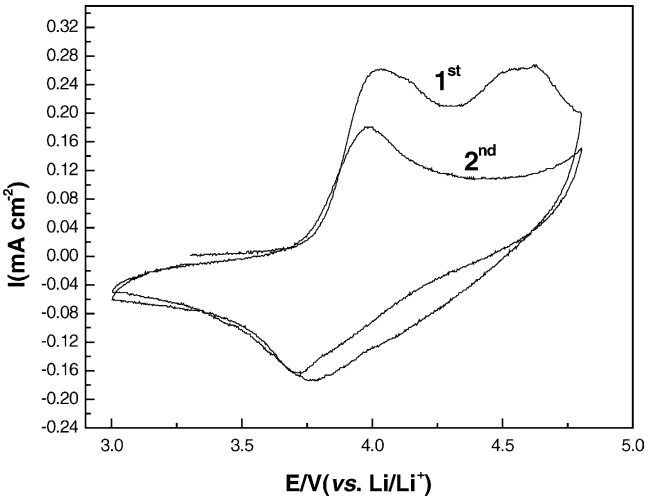

Fig. 5. Cyclic voltammogram of $LiNi_{0.5}Mn_{0.35}Ti_{0.15}O_2$ measured at a scan rate of 0.05 mV/s.

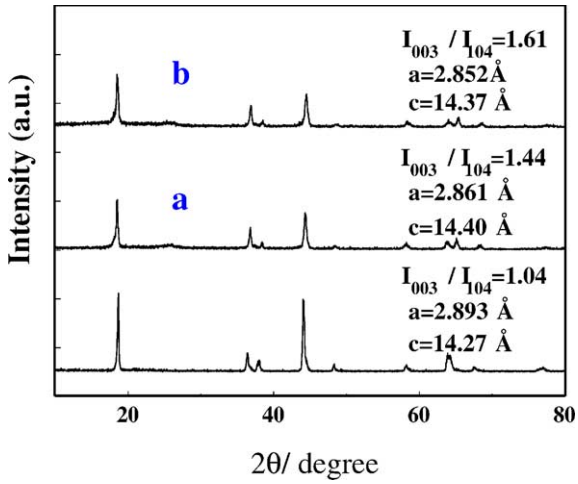

Fig. 6. XRD patterns of charged $LiNi_{0.5}Mn_{0.4}Ti_{0.1}O_2$ cathode: (a) charged to 150 mAh/g; (b) charged to 210 mAh/g.

the existence of 4.6 V plateau in $0.95LiNi_{0.5}Mn_{0.5}O_2 \cdot 0.05Li_2TiO_3$.

Fig. 5 shows the cyclic voltammogram of $LiNi_{0.5}Mn_{0.35}Ti_{0.15}O_2$ measured at a scan rate of 0.05 mV/s. Two anodic peaks are observed in the first oxidation process. One is centered at ca. 4.0 V and the other is centered at ca. 4.6 V. However, only one cathodic peak centered at ca. 3.8 V can be clearly observed in the first reduction process. In the consecutive cycle, only one anodic peak and one cathodic peak appear. The anodic peak centered at ca. 3.95 V and the cathodic peak centered at 3.7 V, slightly lower than that of in first cycle.

In order to elucidate the origin of these two plateaus, ex situ XRD were carried out and the XRD patterns of $LiNi_{0.5}Mn_{0.4}Ti_{0.1}O_2$ cathode charged to different capacities were presented in Fig. 6. The corresponding lattice parameters were also indicted on the XRD profiles. The charged electrode shows the same XRD patterns as the pristine electrode, which means that the layered structure of active material remains unaffected during the charge process. At the charge depth of 150 mAh/g (about 4.4 V), the lattice parameter *a* reduces from 2.893 to 2.861 Å while parameter *c* increase from 14.27 to 14.40 Å. Such change in the lattice parameters is similar to that of $LiNiO_2$ [15]. Further charge to 210 mAh/g (4.8 V) gives rise to the shrinkage of both *a* and *c* axis. Therefore, the process of lithium extraction from lattice is existing in the plateau of 4.6 V.

Fig. 7 shows the discharge capacities of $LiNi_{0.5}Mn_{0.5-x}Ti_xO_2$ ($0 \leq x \leq 0.2$) versus cycle number. All compounds exhibit good cyclability at room temperature. Moreover, the discharge capacity of all compounds varies with cycle number. It is assumed that the capacity fluctuation would

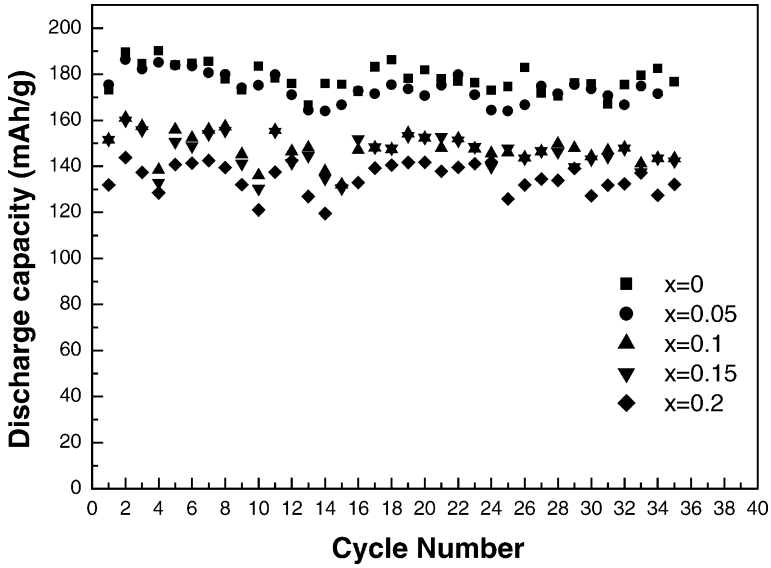

Fig. 7. Discharge capacities of $LiNi_{0.5}Mn_{0.5-x}Ti_xO_2$ ($0 \leq x \leq 0.2$) vs. cycle number operated at room temperature.

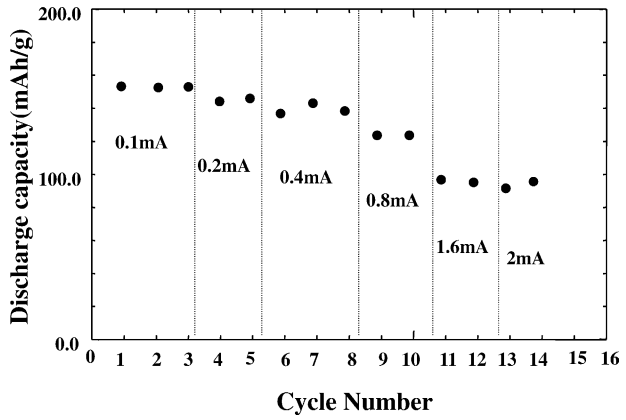

Fig. 8. Rate performance of $LiNi_{0.5}Mn_{0.4}Ti_{0.1}O_2$ vs. cycle number at different discharge current densities.

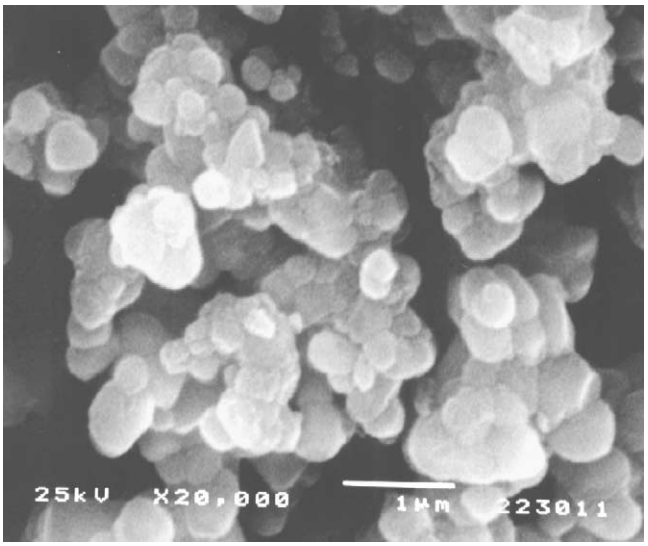

Fig. 9. SEM micrograph of $LiNi_{0.4}Mn_{0.4}Ti_{0.1}O_2$.

be related to the variation of room temperature. This phenomenon has already been reported by Kim et al. [10] and Lu et al. [5]. It is interesting to note that the magnitude of the capacity deviation increases with Ti content increasing, implying that this temperature-dependence is possibly related to the cation mixing.

Fig. 8 shows the rate performance of $LiNi_{0.5}Mn_{0.4}Ti_{0.1}O_2$. The cell was charged to 4.8 V at a rate of 0.1 mA/cm^2 (10 mA/g) and held at 4.8 V for 3 h followed by discharged at different rates to 3 V. The discharge capacity decreases as the discharge current density increases. The rate ability is not very good and the discharge capacity is less than 100 mAh/g at the discharge rate of 2 mA/cm^2 (200 mA/g). The morphology of $LiNi_{0.4}Mn_{0.4}Ti_{0.1}O_2$ is shown in Fig. 9. The compound has a smooth, well-shaped and particle-agglomerated morphology. The average size of primary particle is about 500 nm. The poor rate ability, therefore, is not related to the particle size or specific surface area. It is assumed that the presence of impurity seems to degrade its rate capability.

4. Conclusions

Our results reveal that $LiNi_{0.5}Mn_{0.5-x}Ti_xO_2$ series can be prepared by this simple solid state method. However, some impurities are observed inside of these compounds. It is assumed that these compounds should be considered as a solid solution system rather than Ti substituted $LiNi_{0.5}Mn_{0.5}O_2$ derivatives. These impurities probably give rise to the presence of an additional plateau around 4.6 V, which is the main source of the irreversible capacity in their first cycle between 3–4.8 V, as well as the poor rate capability. We also observed this phenomenon in $LiNi_{1/3}Mn_{1/3}Co_{1/3}O_2$ obtained by different methods [18].

References

[1] J.R. Dahn, U. von Sacken, M.W. Juzkow, H. Al-Janaby, J. Electrochem. Soc. 138 (1991) 2207.
[2] J.M. Tarascon, D. Guyomard, G.L. Baker, J. Power Sources 43/44 (1993) 689.
[3] J.N. Reimers, E.W. Fuller, E. Rossen, J.R. Dahn, J. Electrochem. Soc. 140 (1993) 3396.
[4] T. Ohzuku, Y. Makimura, Chem. Lett. 2001 (2001) 744.
[5] Z. Lu, D.D. MacNeil, J.R. Dahn, Electrochem. Solid State Lett. 4 (2001) A191.
[6] B.L. Cushing, J.B. Goodenough, Solid State Sci. 4 (2002) 1487.
[7] R. Koksbang, J. Barker, H. Shi, M.Y. Saïdi, Solid State Ionics 84 (1996) 1.
[8] W.-S. Yoon, Y. Paik, X.-Q. Yang, M. Balasubramanian, J. McBreen, C.P. Grey, Electrochem. Solid State Lett. 5 (2002) A263.
[9] S.-H. Kang, J. Kim, M.E. Stoll, D. Abraham, Y.K. Sun, K. Amine, J. Power Sources 112 (2002) 41.
[10] J.-S. Kim, C.S. Johnson, M.M. Thackeray, Electrochem. Commun. 4 (2002) 205.
[11] D.D. MacNeil, Z. Lu, J.R. Dahn, J. Electrochem. Soc. 149 (2002) A1332.
[12] E. Rossen, C.D.W. Jones, J.R. Dahn, Solid State Ionics 57 (1992) 311.
[13] D. Li, H. Noguchi, ITE Lett. 4 (2003) 303.
[14] D. Li, H. Noguchi, M. Yoshio, Electrochim. Acta, Submitted for publication.
[15] T. Ohzuku, A. Ueda, M. Nagayama, J. Electrochem. Soc. 140 (1993) 1862.
[16] R.C. Weast, Handbook of Chemistry and Physics, 68th ed., CRC Press, 1987, F157.
[17] M. Yoshio, Y. Todorov, K. Yamato, H. Noguchi, J. Itoh, M. Okada, T. Mouri, J. Power Sources 74 (1998) 46.
[18] D. Li, T. Muta, L. Zhang, M. Yoshio, H. Noguchi, J. Power Sources 132 (2004) 150.